Acta Pharm. *58* (2008) 335–345
10.2478/v10007-008-0020-5

Short communication

3D-QSAR studies for the binding affinity toward (*R,S*)-2-amino-3-(3-hydroxy-5-methylisoxazol-4-yl)--propionic acid receptor

RITESH N. SHARMA[1*]
HARDIK THAKAR[2]
KAMALA K. VASU[2]
SUBHASH C. CHATURVEDI[3]

[1] *S. K. Patel College of Pharmaceutical Education and Research, Ganpat University Kherva-382711 Gujarat, India*

[2] *B. V. Patel Pharmaceutical Education and Research Development (PERD) Centre Thaltej-Gandhinagar Highway Thaltej Ahmedabad-380054 Gujarat, India*

[3] *School of Pharmacy, Devi Ahilya Vishwavidyalaya, Indore-452017 M.P., India*

Accepted July 24, 2008

An approach for binding affinity evaluation is suggested and exemplified using a set of triazolo [1,5-a] quinoxaline for the *(R,S)*-2-amino-3-(3-hydroxy-5-methylisoxazol--4-yl)-propionic acid (AMPA) receptor. Biological activity toward the AMPA receptor (expressed as –log IC_{50}) was taken as a dependent variable for building Comparative Molecular Field Analysis (CoMFA) and Comparative Molecular Similarity Indices Analysis (CoMSIA) models. The resulting models show the ways of increasing the binding affinity to the AMPA receptor as a potential target for epilepsy. The statistically significant results show that the cross-validated r^2_{CV} value (0.766) for the CoMFA model is greater than (0.758) for the CoMSIA model. The non-cross validated run giving the coefficient of determination r^2 values of 0.944 and 0.919 for CoMFA and CoMSIA, respectively, provided good correlation between the observed and computed affinities of the training set compounds. The resulting CoMFA and CoMSIA models indicate that steric, electrostatic, hydrophobic (lipophilic), hydrogen bond donor and acceptor substituents play a significant role in increasing the binding affinity and selectivity of the compounds toward the AMPA receptor.

Endogenous ligand (*S*)-glutamate (Glu) is a major excitatory neurotransmitter in the central nervous system (CNS), which is responsible for basal excitatory synaptic transmission and many forms of synaptic plasticity. On the other hand, glutamatergic hyperactivity may lead to neurotoxicity. In fact, excessive endogenous glutamate is implicated in a number of acute and chronic neurodegenerative pathologies such as epilepsy, cerebral ischaemia and Parkinson's diseases (1). Glutamate activates specific receptors that belong to the classes of metabotropic receptors (mGluRs, coupled to G-protein) and ionotropic receptors (iGluRs, ligandgated ion channel). The latter are divided into the *N*-methyl-D-aspartic acid (NMDA) receptor, the kainic acid (KA) receptor and the *(R,S)*-2-amino-3-(3-hydroxy-5-methylisoxazol-4-yl)-propionic acid (AMPA) receptor (2, 3).

* Correspondence; e-mail address: riteshn.sharma@gmail.com

In this paper, AMPA receptor will be described as a potential target for convulsive therapeutic intervention. Different series of compounds with inhibitory activity toward the AMPA receptor have been developed. Most of these inhibitors are structurally derived from AMPA, quinoxaline, quinoxalinedione or 2,3-benzodiazepine (1, 4–9). Early studies showed that AMPA receptor antagonists were capable of blocking seizures in rodent models of epilepsy (10, 11). In spite of their promising anticonvulsant activity in various animal model studies, no AMPA receptor inhibitors are in clinical use against epilepsy today. Thus, AMPA can be considered a potential target for therapeutic prevention of epileptic seizure (8, 12). Hence, we have the proposed an approach for increasing the binding affinity of ligands toward AMPA receptor that may help in the treatment of convulsive disorders.

Comparative molecular field analysis (CoMFA) (13) and comparative molecular similarity indices analysis (CoMSIA) (14) are widely used tools for predicting biological activity of ligands. They enable designing novel ligands with enhanced affinity to a given receptor. To study the binding affinity, a set of triazolo [1,5-a] quinoxaline with biological activities expressed as IC_{50}, *i.e.*, the concentration necessary for 50% AMPA receptor inhibition, was taken as a dependent variable for building CoMFA and CoMSIA models. The resulting model would directly suggest the ways of increasing the binding affinity for AMPA receptor.

EXPERIMENTAL

Dataset for the study

Reported *in vitro* AMPA receptor inhibition data on a series of triazolo [1,5-a] quinoxaline derivatives were used for this study (Table I) (15–18). The IC_{50} values of 35 molecules were segregated into groups of 30 and 5 as a training set and a test set, respectively. To achieve data homogeneity, K_i (μmol L^{-1}) values were converted to IC_{50} (μmol L^{-1}) by the Cheng-Prusoff equation (19) and then all IC_{50} values were converted to pIC_{50}.

Molecular modeling

The 3D-QSAR was performed using the SYBYL (Tripos Inc., USA) version 6.9 installed on an IBM server and Linux operating system. The most active analogue was subjected to conformational search. The least energy conformer thus obtained as bioactive conformation was taken as the template and the remaining molecules were built from it. The geometry of all molecules was optimized using the tripose force field and Powell's conjugated gradient with the Gasteiger-Hückel charges. The minimum energy difference of 4.19 J mol^{-1} was set as convergence criterion.

Alignment

CoMFA and CoMSIA studies require the coordinate of a molecule to be aligned according to reasonable bioactive conformation. All the molecules were aligned with respect to template molecule **22** by the *Atom Fit* method in the SYBYL (version 6.9) molecular modeling software to ensure pharmacophore matching. The alignment of molecules is shown in Fig. 1a.

Table I. Molecules used in the 3D-QSAR analysis

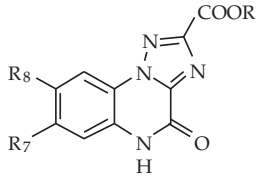

Molecule No.	R	R_8	R_7	Biological activity (pIC_{50})			Ref.
				Actual	Predicted		
					CoMFA	CoMSIA (ALL)	
			Training set				
1	H	NO_2	Cl	–0.18	–0.34	–0.56	15
2	Et	1*H*-imidazol-1-yl	Cl	–0.47	–0.42	–0.31	15
3	H	1*H*-imidazol-1-yl	Cl	–0.10	0.36	–0.01	15
4	Et	4*H*-1,2,4-triazol-4-yl	Cl	0.04	0.26	0.04	15
5	H	4*H*-1,2,4-triazol-4-yl	Cl	0.74	0.58	0.58	15
6	Et	4H-1,2,4-triazol-4-yl	CF_3	0.58	0.56	0.62	16
7	H	4*H*-1,2,4-triazol-4-yl	CF_3	0.91	0.93	1.08	16
8	Et	3-formyl-1*H*-pyrrol-1-yl	CF_3	0.32	-0.07	0.01	16
9	H	3-formyl-1*H*-pyrrol-1-yl	CF_3	0.81	0.61	0.63	16
10	Et	1*H*-pyrrol-1-yl	CF_3	–0.45	–0.20	–0.33	16
11	H	1*H*-pyrrol-1-yl	CF_3	0.44	0.38	0.34	16
12	Et	3-carboxy-1*H*-pyrrol-1-yl	CF_3	0.34	0.46	0.55	16
13	H	3-carboxy-1*H*-pyrrol-1-yl	CF_3	1.32	1.26	1.24	16
14	Et	3-formyl-2,5-dioxo-2,5-dihydro-1*H*-pyrrol-1-yl	CF_3	–1.21	–1.41	–1.12	16
15	Et	1*H*-imidazol-1-yl	CF_3	0.34	0.09	0.02	16
16	H	1*H*-imidazol-1-yl	CF_3	0.81	0.71	0.77	16
17	Et	3-formyl-1*H*-pyrrol-1-yl	NO_2	0.07	0.13	0.08	16
18	H	3-formyl-1*H*-pyrrol-1-yl	NO_2	0.63	0.68	0.88	16
19	Et	1*H*-pyrrol-1-yl	NO_2	–0.25	–0.33	0.06	16
20	H	1*H*-pyrrol-1-yl	NO_2	0.94	0.77	0.53	16
21	Et	3-carboxy-1*H*-pyrrol-1-yl	NO_2	1.05	1.09	0.88	16
22	H	3-carboxy-1*H*-pyrrol-1-yl	NO_2	1.61	1.31	1.64	16
23	Et	NO2	CF_3	–1.06	–0.83	–1.16	16
24	H	NO_2	CF_3	–0.48	–0.47	–0.70	16
25	Et	NH_2	CF_3	–0.84	–0.68	–0.75	16
26	H	NH_2	CF_3	–0.18	–0.24	–0.12	16
27	Et	$NHCOCH_3$	NO_2	–0.92	–0.97	–0.88	16
28	H	$NHCOCH_3$	NO_2	–0.25	–0.16	–0.42	16

29	Et	NH_2	NO_2	–0.18	–0.21	–0.32	16
30	H	NH_2	NO_2	0.04	0.25	0.15	16
			Test set				
31	H	H	4*H*-1,2,4-triazol-4-yl	–0.74	–0.71	–0.46	17
32	Et	H	4*H*-1,2,4-triazol-4-yl	–1.11	–0.41	–0.11	17
33	H	3-formyl-1*H*-pyrrol-1-yl	Cl	0.16	0.62	0.16	17
34	Et	3-formyl-1*H*-pyrrol-1-yl	Cl	–0.38	–0.79	–0.33	17
35	H	H	H	–	–0.04	–0.19	18

CoMFA interaction energy

The van der Waals potential and Coulombic term representing the steric and electrostatic field, respectively, was calculated using standard tripose force fields. A distance dependent dielectric constant was used. An sp^3 carbon with a charge of +1 served as a probe atom. CoMFA field descriptors were calculated at each lattice interaction of a regular space of 2.0×10^{-10} m in all three dimensions within the defined region. The steric and electrostatic fields were truncated at ± 125.6 kJ mol^{-1}. CoMFA QSAR equations were derived with the partial least squares (PLS) algorithm.

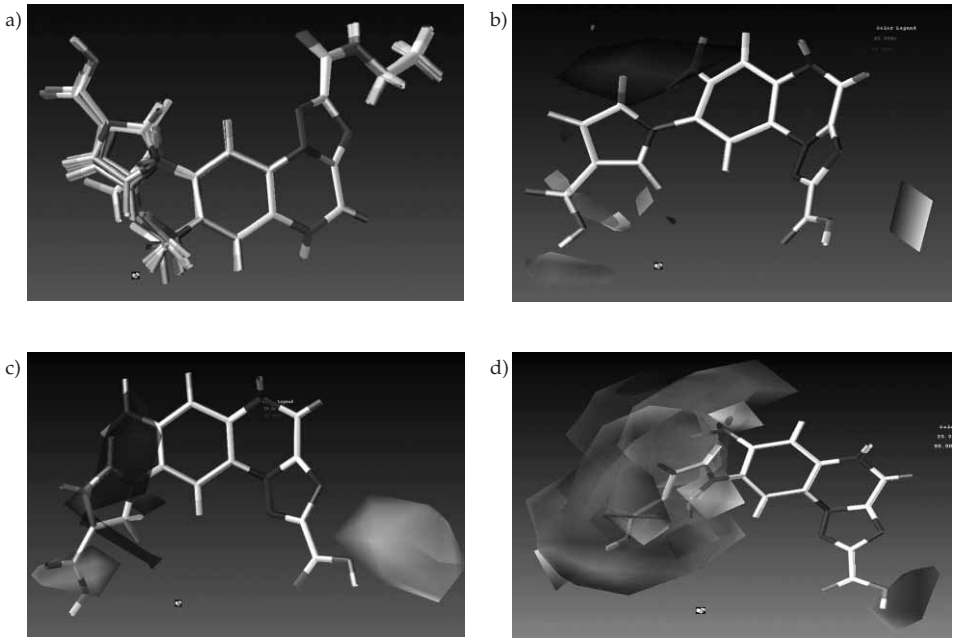

Fig. 1. a) Alignment of triazolo[1,5-a]quinoxaline molecules; b) CoMFA STDEV*COEFF contour maps for steric and electrostatic fields; CoMSIA STDEV*COEFF contour maps for c) steric and electrostatic fields; d) hydrophobic, donor and acceptor fields, of AMPA model. The most active molecule **22** is displayed in the background.

CoMSIA interaction energy

The recently reported CoMSIA method is based on molecular similarity descriptors. CoMSIA calculates the similarity descriptors by way of a grid lattice. For a molecule j with atoms i at the grid point q, the CoMSIA similarity indices A_F are calculated by the equation as follows:

$$A_F^q(j) = -\sum \omega_{probe.k}\omega_{ik}exp(\alpha_{iq}^{r2})$$

where ω_{ik} is the actual value of the physicochemical property k of atom i, $\omega_{probe.k}$ is the property of the probe atom with pre-set charge (+1 in this case), radius (1.53×10^{-10} m), and hydrophobicity of 1 and r_{iq} is the mutual distance between the probe atom at grid point q and atom i of the molecule. In CoMSIA calculations, five physicochemical properties (steric, electrostatic, hydrophobic, hydrogen bond donor, and hydrogen bond acceptor) were determined for all molecules. The attenuation factor value was set to 0.3. Similarity descriptors can be calculated at all grid points inside as well as outside the molecule. This generally follows the CoMFA protocols and is evaluated by PLS analysis.

PLS analysis

Partial Least Squares analysis (PLA) was performed to obtain a 3D-QSAR model after all of the CoMFA and CoMSIA descriptors were calculated. The PLS method was used to correlate the activity (dependent variable) with various physicochemical properties (independent variables). The CoMFA and CoMSIA standard scaling and column filtering of 0.5 were used in PLS analysis.

Cross-validations in PLS were done by the leave-one-out procedure to find out the optimal number of components in building regression models and to check statistic significance of the models. The leave-one-out technique provides a good way to quantitatively evaluate the internal predictive ability of a model by removing one compound at a time and then building the QSAR model and calculating the activity of the compound using the new model constructed from the remaining compounds in the data set.

The high value of the cross-validated coefficient of determination (r^2_{CV}) and the lowest standard error of prediction resulted in optimum number of components considered for further analysis. The optimal number of components obtained is then used to derive the final QSAR model using all the compounds (without cross-validation). The conventional coefficient of determination (r^2) and F value are used to measure the quality of the model.

RESULTS AND DISCUSSION

QSAR model

CoMFA and CoMSIA models were values with derivatives of triazolo [1,5-a] quinoxaline from inhibition values (pIC_{50}) with respect to the AMPA receptor. Various 3D--QSAR (CoMFA and CoMSIA) models were generated and the best one was selected using the statistically significant parameters. Actual and predicted values obtained after the CoMFA and CoMSIA analysis of training and test molecules are given in Table I.

The PLS analysis for a different number of components was tried using 0.0 kJ mol^{-1} column filtering value for CoMFA and CoMSIA models. Based on better statistical values, the optimum number of components were selected. For the CoMFA model, the cross--validated coefficient of determination (r^2_{CV}) = 0.766 with five components, non cross--validated coefficient of determination (r^2) = 0.944, *F* value = 80.23 and boot straped r^2 = 0.953 were determined. The values of the standard error of estimate (SEE) and the predicted residual sum of squares (PRESS) obtained for CoMFA were 0.187 and 0.48, repectively.

The CoMSIA results were obtained using the same alignment and the same training set molecules. As depicted in Table II, individual models were developed for CoMSIA analysis taking different combinations of fields, *i.e.*, steric-electrostatic (S-E), steric-electrostatic-hydrophobic (S-E-H), steric-electrostatic-hydrogen bond donor-hydrogen bond acceptor (S-E-D-A) and using all (S-E-D-A-H) fields. Out of these, the model having a combination of S, E, D, A fields was slightly better than other models. However, the all--field model is the one providing the most descriptive information and hence was used for the prediction of training and test set molecules. The cross-validated r^2_{CV} = 0.758

Table II. The comparative PLS statistic results

Parameter	CoMFA	CoMSIA			
		S,E	S,E,H	S,E,D,A	ALL
r^2_{CV}	0.766	0.712	0.617	0.760	0.758
N	5	6	5	5	5
SEP	0.355	0.387	0.401	0.359	0.361
r^2 boot strap	0.953	0.954	0.920	0.965	0.937
r^2	0.944	0.920	0.855	0.920	0.919
SEE	0.187	0.227	0.299	0.222	0.223
F value	80.23	44.01	28.24	55.40	54.75
Probalityof $r^2 = 0$	0.00	0.00	0.00	0.00	0.00
PRESS	0.48	0.62	0.53	0.59	0.67
		Contribution (%)			
Steric	0.545	0.311	0.200	0.096	0.066
Electrostatic	0.455	0.689	0.510	0.337	0.250
Hydrophobic			0.290		0.228
Donor				0.263	0.189
Acceptor				0.304	0.267

r^2_{CV} – cross-validated coefficient of determination.
N – No. of components.
SEP – standard error of prediction.
r^2 boot strap – coefficient of determination to boot strap run.
r^2 – conventional coefficient of determination.
SEE – standard error of estimate.
PRESS – Predicted residual sum of square.
S – Steric field, E – Electrostatic field, H – hydrophobic field, D – hydrogen bond donor field, A – hydrogen bond acceptor field.

with five components, non cross-validated $r^2 = 0.919$, F value = 54.75 and boot strapped $r^2 = 0.937$ were obtained from the CoMSIA all-field model. The values of the standard error of estimate (SEE) and the predicted residual sum of squares (PRESS) obtained for the CoMSIA all-field model were 0.223 and 0.67, respectively. Correlation between the predicted activity and actual activity toward the AMPA receptor obtained from the CoMFA and CoMSIA study is illustrated in Fig. 2. The correlation coefficient, between actual activity and predicted activity of 0.967 and 0.965 for CoMFA and CoMSIA all-field models, respectively, explain the good predictability of both models.

The comparative study data (Table II) of CoMFA and CoMSIA models shows that the cross-validated r^2_{CV} and non cross-validated r^2 from CoMFA is slightly higher than the CoMSIA all-field model and SEDA model. All statistical parameters, *i.e.*, F value, SEE, and SEP suggest that the CoMFA model is slightly better than the CoMSIA model for prediction of training and test set molecules.

CoMFA and CoMSIA calculate the electrostatic, steric, hydrophobic, hydrogen bond donor and acceptor properties based on the grid built around the molecules. The results prove that steric and electrostatic contributions are apparently different for CoMFA (0.545 and 0.455) as compared to the CoMSIA (0.066 and 0.250) model. CoMFA model shows nearly equal significance of steric and electrostatic properties while the electrostatic contribution in the CoMSIA model is almost three fold that of the steric contribution, indicating the importance of the electrostatic field in model generation. The remaining fields, like hydrophobic, hydrogen bond donor and acceptor, are virtually equal contributors in the CoMSIA models. Since CoMFA and CoMSIA models have almost equal statistically significant parameters, either CoMFA or CoMSIA model could be used for prediction of training and test set molecules. However, CoMSIA can be preferred to explain the importance of hydrophobic, hydrogen bond donor and acceptor properties together with stereo-electric parameters. For external validation, test molecules were selected to include a variety of substituents at positions R_7 and R_8 and to have triazolo [1,5-a] quinoxaline as a common molecular scaffold. Prediction of test molecules was obtained from CoMFA and CoMSIA models (Table I) with predicted residual sum of squares (PRESS) values of 0.547 and 1.298, respectively.

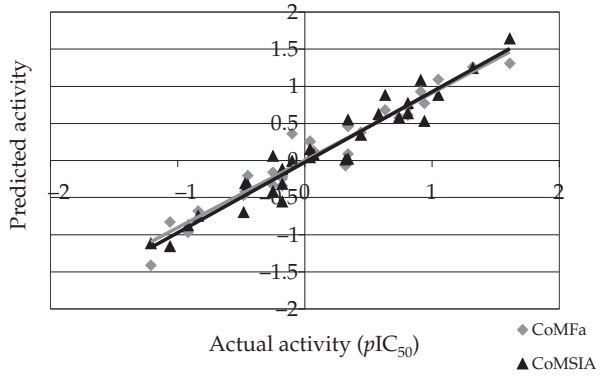

Fig. 2. Correlation of predicted activity *vs*. actual activity toward the AMPA receptor.

Graphical interpretation of results

3D-QSAR models depict the change in binding preference occurring upon the change in molecular fields around ligands. Compound **22** (template), the most active molecule of the series, is used for the presentation of contour maps. In the case illustrated in Fig. 1b, for CoMFA, a sterically favorable contour near the 1*H*-pyrrole-3-carboxylic acid group at position 8 and a heavy electropositive favorable contour at position R_7 of the triazolo [1,5-a] quinoxaline ring were found. They suggest that modification of the carboxylic group, specifically on heterocyclic substituents at position 8, and addition of the positively charged group at position R_7 would increase the binding affinity for the AMPA receptor. It is evident from the example that molecule **13** 1*H*-pyrrole-3-carboxylic acid substituent is more active for the AMPA receptor than molecule **9** with 1*H*-pyrrole--3-carbaldehyde substituent at R_8.

For CoMSIA (Fig. 1c), the stereo-electric contours are similar to CoMFA, excluding the small sterically unfavorable contour at the second position of quinoxaline ring. This illustrates the significance of the carboxyl group rather than ethyl ester at the second position of quinoxalmiering for increasing the affinity. The two contour maps for bulky and positively charged regions, respectively, are major contributors, impling the presence of bulky electropositively charged substituents at positions 7 and 8 which might also increase the binding affinity, *e.g.*, in molecule **22**. In Fig. 1d, the unfavorable hydrogen bond donor and hydrogen bond acceptor contour maps share a major portion at R_7 and R_8 of the quinoxaline ring, indicating that absence of hydrogen bond donor and acceptor groups near R_7 and R_8, respectively, may be responsible for increasing the binding affinity. One hydrogen bond donor favorable contour close to 1*H*-pyrrole-3-carboxylic acid group at position 8 of the quinoxaline ring suggests that the hydrogen bond donor group at this position will possibly increase the binding affinity. Favorable hydrophobic contours on CF_3 group at position 7 and the favorable hydrophobic small contour on the pyrole ring attached to position 8 of quinoxaline scaffold recommends the presence of the hydrophobic group or the hydrophilic group, for increasing affinity. Thus, CoMFA and CoMSIA models suggest that by modifying the structure of ligands, particularly at positions R_7 and R_8, one could gain higher affinity toward the AMPA receptor.

CONCLUSIONS

The 3D-QSAR analysis makes it possible to relate chemical structures of ligands and their binding affinity with respect to different bio targets by using the CoMFA and CoMSIA techniques. This provides a direct view of the factors expressed in terms of CoMFA and CoMSIA molecular fields (electrostatic, steric, hydrophobic, hydrogen bond donor and acceptor) affecting the binding affinity, which in turn žcould give a reasonably good prediction of binding affinity.

Finally, this analysis is helpful in suggesting some structural modifications in known compounds for designing novel ligands, more effective as anticonvulsive agents.

Acknowledgements. – The author wishes to thank Dr. Harish Padh, Director, B. V. Patel Pharmaceutical Education and Research Development (PERD) Center, for providing the software facility. This work was supported by the junior research fellowship awarded by the All India Council of Technical Education (AICTE) to the author.

REFERENCES

1. H. Bräuner-Osborne, J. Egebjerg, E. Ø. Nielsen, U. Madsen and P. Krogsgaard-Larsen, Ligands for glutamate receptor: Design and therapeutic prospects, *J. Med. Chem.* **43** (2000) 2609–2645; DOI: 10.1021/jm000007r.
2. R. Dingledine, K. Borges, D. Bowie and S. F. Traynelis, The glutamate receptor ion channels, *Pharmacol. Rev.* **51** (1999) 7–61.
3. M. Hollmann and S. Heinemann, Cloned glutamate receptors, *Annu. Rev. Neurosci.* **17** (1994) 103–108.
4. G. J. Lees, Pharmacology of AMPA/kainate receptor ligands and their therapeutic potential in neurological and psychiatric disorders, *Drugs* **59** (2000) 33–78; DOI: 10.2165/00003495-200059010--00004.
5. U. Madsen, T. B. Stensbøl and P. Krogsgaard-Larsen, Inhibitors of AMPA and kainate receptors, *Curr. Med. Chem.* **8** (2001) 1291–1301.
6. S. S. Nikam and B. E. Kornberg, AMPA receptor antagonists, *Curr. Med. Chem.* **8** (2001) 155–170.
7. T. B. Stensbøl, U. Madsen and P. Krogsgaard-Larsen, The AMPA receptor binding site: Focus on agonists and competitive antagonists, *Curr. Pharm. Des.* **8** (2002) 857–872; DOI: 10.2174/1 381612024607090.
8. Y. P. Auberson, Competitive AMPA antagonism: A novel mechanism for antiepileptic drugs, *Drugs Fut.* **26** (2001) 463–471; DOI: 10.1358/dof.2001.026. 05.659545.
9. S. D. Donevan and M. Rogawski, GYKI 52466, a 2,3-benzodiazepine, is a highly selective, non-competitive antagonist of AMPA/kainate receptor responses, *Neuron* **10** (1993) 51–59; DOI: 10.1016/0896–6273(93)90241-I.
10. A. Tortorella, T. Halonen, N. Sahibzada and K. Gale, A crucial role of the α-amino-3-hydroxy--5-methylisoxazole-4-propionic acid subtype of glutamate receptors in piriform and perirhinal cortex for the initiation and propagation of limbic motor seizures, *J. Pharmacol. Exp. Ther.* **280** (1997) 1401–1405.
11. W. Löscher, Pharmacology of glutamate receptor antagonists in the kindling model of epilepsy, *Prog. Neurobiol.* **54** (1998) 721–741; DOI: 10.1016/S0301-0082(97)00092-0.
12. W. Loscher, H. Lehmann, B. Behl, D. Seemann, H. J. Teschendorf, H. P. Hofmann, W. Lubisch, T. Hoger, H. G. Lemaire and G. Gross, A new pyrrolyl-quinoxalinedione series of non-NMDA glutamate receptor antagonists: pharmacological characterization and comparison with NBQX and valproate in the kindling model of epilepsy, *Eur. J. Neurosci.* **11** (1999) 250–262; DOI: 10.1046/ j.1460-9568.1999.00432.x.
13. G. R. Desraju, B. Gopalakrishnan, R. K. Jetti, A. Nagarjun, D. Raveendra, J. A. Sarma, M. E. Sobhia and R. Thiagavathi, Computer-aided design of selective cox-2 inhibitors: comparative molecular field analysis, comparative molecular similarity indices analysis, and docking studies of some 1,2-diarylimidazole derivatives, *J. Med. Chem.* **45** (2002); DOI: 10.1021/jm020198t.
14. M. T. Bohm. J. Sturzebecher and G. Klebe, Three dimensional quantitative structure activity relationship analysis using comparative molecular field analysis and comparative molecular similarity search analysis to elucidate selectivity differences of inhibitor binding to trypsin, thrombin and factor Xa, *J. Med. Chem.* **42** (1999) 458–477; DOI: 10.1021/jm981062r.
15. D. Catarzi, V. Colotta, F. Varano, L. Cecchi, G. Filacchioni, A. Galli, C. Costagli and V. Carla, 7-Chloro-4,5-dihydro-8-(1,2,4-triazole-4-yl)-4-oxo-1,2,4-triazolo[1,5-a] quinoxaline-2-carboxylates as novel highly selective AMPA receptor antagonists, *J. Med. Chem.* **43** (2000) 3824–3826; DOI: 10.1021/jm0009686.
16. D. Catarzi, V. Colotta, F. Varano, L. Cecchi, G. Filacchioni, V. R. Calabri, A. Galli, C. Costagli and V. Carla, Synthesis and biological evaluation of analogues of 7-chloro-4,5-dihydro-4-oxo-8--(1,2,4-triazol-4-yl)-1,2,4-triazolo[1,5-*a*] quinox -aline-2-carboxylic acid (TQX-173) as novel selective AMPA receptor antagonists, *J. Med. Chem.* **47** (2004) 262–272; DOI: 10.1021/jm030906q.

17. D. Catarzi, V. Colotta, F. Varano, L. Cecchi, G. Filacchioni, A. Galli, C. Costagli and V. Carla, Synthesis, ionotropic glutamate receptor binding affinity, and structure-activity relationships of a new set of 4,5-dihydro-8-heteroaryl-4-oxo-1,2,4-triazolo[1,5-*a*] quinoxaline-2-carboxylates analogues of TQX-173, *J. Med. Chem.* **44** (2001) 3157–3165; DOI: 10.1021/jm010862q.
18. F. Varano, D. Catarzi, V. Colotta, G. Filacchioni, A. Galli, C. Costagli and V. Carla, Synthesis and biological evaluation of a new set of pyrazolo[1,5-*c*]quinazoline-2-carboxylates as novel excitatory amino acid antagonists, *J. Med. Chem.* **45** (2002) 1035–1044; DOI: 10.1021/jm010995b.
19. Y. C. Cheng and W. H. Prusoff, Relationship between the inhibition constant (*Ki*) and the concentration of inhibitor which causes 50% inhibition (IC_{50}) of an enzymatic reaction, *Biochem. Pharmacol.* **22** (1973) 3099–3108; DOI: 10.1016/0006-2952(73)90196-2.

S A Ž E T A K

3D-QSAR studija za afinitet vezanja na receptor za *(R,S)*-2-amino-3-(3-hidroksi-5-metilizoksazol-4-il)-propansku kiselinu

RITESH N. SHARMA, HARDIK THAKAR, KAMALA K. VASU i SUBHASH C. CHATURVEDI

U radu je vrednovan afinitet vezanja serije triazolo[1,5-a]kinoksalina na receptor za *(R,S)*-2-amino-3-(3-hidroksi-5-metilizoksazol-4-il)-propansku kiselinu (AMPA). Djelovanje na AMPA receptor (izraženo kao –log IC_{50}) uzeta je kao zavisna varijabla u modelima usporedne analize molekulskih polja (*Comparative Molecular Field Analysis*, CoMFA) i usporedne analize molekulske sličnosti (*Comparative Molecular Similarity Indices Analysis*, CoMSIA). Ti modeli pokazuju kako povećati afinitet vezanja na AMPA receptor, što može biti korisno u terapiji epilepsije. Statistički značajni rezultati ukazuju da je križno validirana r^2_{CV} vrijednost za CoMFA model (0,766) veća nego za CoMSIA model (0,758). Koeficijenti r^2 za CoMFA model (0,944) i CoMSIA (0,919) ukazuju na dobru korelaciju između izračunatih i eksperimentalno određanih afiniteta vezanja proučavane serije spojeva. Prema oba modela za povećanje afiniteta vezanja i selektivnost spojeva za AMPA receptor značajna su sterička, elektrostatska, hidrofobna (lipofilni) svojstva, te sposobnost stvaranja vodikovih veza.

Ključne riječi: afinitet vezanja, 3D-QSAR, CoMFA, CoMSIA, AMPA receptor

S. K. Patel College of Pharmaceutical Education and Research, Ganpat University, Kherva-382711, Gujarat, India

B. V. Patel Pharmaceutical Education and Research Development (PERD) Centre, Thaltej-Gandhinagar Highway, Thaltej, Ahmedaba-380054, Gujarat, India

School of Pharmacy, Devi Ahilya Vishwavidyalaya, Indore-452017, M.P., India

Supporting information: Smile structures of all compounds

Molecule	Smile structure
1	O=C(O)c3nc2c(=O)[nH]c1cc(Cl)c(N(=O)=O)cc1n2n3
2	CCOC(=O)c4nc3c(=O)[nH]c2cc(Cl)c(n1ccnc1)cc2n3n4
3	O=C(O)c4nc3c(=O)[nH]c2cc(Cl)c(n1ccnc1)cc2n3n4
4	CCOC(=O)c4nc3c(=O)[nH]c2cc(Cl)c(n1cnnc1)cc2n3n4
5	O=C(O)c4nc3c(=O)[nH]c2cc(Cl)c(n1cnnc1)cc2n3n4
6	CCOC(=O)c4nc3c(=O)[nH]c2cc(C(F)(F)F)c(n1cnnc1)cc2n3n4
7	O=C(O)c4nc3c(=O)[nH]c2cc(C(F)(F)F)c(n1cnnc1)cc2n3n4
8	CCOC(=O)c4nc3c(=O)[nH]c2cc(C(F)(F)F)c(n1ccc(C=O)c1)cc2n3n4
9	O=Cc4ccn(c1cc2c(cc1C(F)(F)F)[nH]c(=O)c3nc(C(=O)O)nn23)c4
10	CCOC(=O)c4nc3c(=O)[nH]c2cc(C(F)(F)F)c(n1cccc1)cc2n3n4
11	O=C(O)c4nc3c(=O)[nH]c2cc(C(F)(F)F)c(n1cccc1)cc2n3n4
12	CCOC(=O)c4nc3c(=O)[nH]c2cc(C(F)(F)F)c(n1ccc(C(=O)O)c1)cc2n3n4
13	O=C(O)c4ccn(c1cc2c(cc1C(F)(F)F)[nH]c(=O)c3nc(C(=O)O)nn23)c4
14	CCOC(=O)c4nc3c(=O)[nH]c2cc(C(F)(F)F)c(N1C(=O)CC(C=O)C1=O)cc2n3n4
15	CCOC(=O)c4nc3c(=O)[nH]c2cc(C(F)(F)F)c(n1ccnc1)cc2n3n4
16	O=C(O)c4nc3c(=O)[nH]c2cc(C(F)(F)F)c(n1ccnc1)cc2n3n4
17	CCOC(=O)c4nc3c(=O)[nH]c2cc(N(=O)=O)c(n1ccc(C=O)c1)cc2n3n4
18	O=Cc4ccn(c1cc2c(cc1N(=O)=O)[nH]c(=O)c3nc(C(=O)O)nn23)c4
19	CCOC(=O)c4nc3c(=O)[nH]c2cc(N(=O)=O)c(n1cccc1)cc2n3n4
20	O=C(O)c4nc3c(=O)[nH]c2cc(N(=O)=O)c(n1cccc1)cc2n3n4
21	CCOC(=O)c4nc3c(=O)[nH]c2cc(N(=O)=O)c(n1ccc(C(=O)O)c1)cc2n3n4
22	O=C(O)c4ccn(c1cc2c(cc1N(=O)=O)[nH]c(=O)c3nc(C(=O)O)nn23)c4
23	CCOC(=O)c4nc3c(=O)[nH]c2cc(C(F)(F)F)c(n1ccc(N(=O)=O)c1)cc2n3n4
24	O=C(O)c4nc3c(=O)[nH]c2cc(C(F)(F)F)c(n1ccc(N(=O)=O)c1)cc2n3n4
25	CCOC(=O)c3nc2c(=O)[nH]c1cc(C(F)(F)F)c(N)cc1n2n3
26	Nc4ccn(c1cc2c(cc1C(F)(F)F)[nH]c(=O)c3nc(C(=O)O)nn23)c4
27	CCOC(=O)c3nc2c(=O)[nH]c1cc(N(=O)=O)c(NC(C)=O)cc1n2n3
28	CC(=O)Nc1cc2c(cc1N(=O)=O)[nH]c(=O)c3nc(C(=O)O)nn23
29	CCOC(=O)c3nc2c(=O)[nH]c1cc(N(=O)=O)c(N)cc1n2n3
30	Nc1cc2c(cc1N(=O)=O)[nH]c(=O)c3nc(C(=O)O)nn23
31	O=C(O)c4nc3c(=O)[nH]c2cc(n1cnnc1)ccc2n3n4
32	CCOC(=O)c4nc3c(=O)[nH]c2cc(n1cnnc1)ccc2n3n4
33	CCOC(=O)c4nc3c(=O)[nH]c2cc(Cl)c(n1ccc(C=O)c1)cc2n3n4
34	Cc4ccn(c1cc2c(cc1Cl)[nH]c(=O)c3nc(C(=O)O)nn23)c4